

nature

INTERNATIONAL WEEKLY JOURNAL OF SCIENCE

Volume 321 No 6069 29 May-4 June 1986 £1.90



SEGMENTATION
GENE CLONED

ASBC
special issue

Isolation of the *paired* gene of *Drosophila* and its spatial expression during early embryogenesis

François Kilchherr, Stefan Baumgartner, Daniel Bopp, Erich Frei & Markus Noll

Department of Cell Biology, Biocenter of the University of Basel, Klingelbergstrasse 70, CH-4056 Basel, Switzerland

We have cloned the paired gene of Drosophila melanogaster, a pair-rule gene required for the establishment of proper segmentation. The transcriptional pattern in young embryos shows developmental polarities along the antero-posterior and dorso-ventral axes. Transcripts, initially expressed with a double-segment periodicity, switch to a single-segment repeat during syncytial blastoderm.

SEGMENTATION, an important process of animal development, is the most conspicuous event of compartmentalization. A systematic search for mutations affecting segmentation in the fruitfly *Drosophila* has revealed that it is governed by ~30 genes which can be divided into four classes according to their mutant phenotypes^{1,2}. In the first class, the gap mutants, various overlapping non-terminal subregions of the larva are deleted. The second class contains the segment-polarity mutants which exhibit defects that are reiterated in every segment; whereas in the third class, the pair-rule mutants, structures are deleted at a two-segment periodicity (Fig. 1). These three classes of mutants suggest that segmentation involves three different units of spatial organization: one of a single-segment periodicity; one of a two-segment periodicity and a third comprising groups of adjacent segments and exhibiting no obvious periodicity. Mutants of the fourth class, the coordinate mutants, are all maternal and show global effects on the segmentation pattern. Their phenotypes have been explained by a defect in the expression of maternal components that regulate the genes of the three other classes^{1,2}.

In *Drosophila*, segmentation becomes visible as early as 1 h after the onset of gastrulation¹. Even earlier, however, during cellular blastoderm, cell lineage may already become restricted to segments³⁻⁷. At the molecular level, this is probably reflected by the spatially restricted expression of the pair-rule gene *fushi tarazu* (*ftz*) at cellular blastoderm, which shows a repetitive pattern of seven evenly spaced bands⁸ that correspond to the primordia of the regions deleted at a two-segment periodicity in homozygous *ftz* mutants^{1,2}. More recently, another pair-rule gene, *hairy* (*h*), has been cloned^{9,10}. Its expression, as analysed by *in situ* hybridization to blastoderm sections, exhibits a pattern of the same periodicity as *ftz* but is shifted anteriorly with respect to *ftz*, by slightly more than one segment primordium¹⁰. In addition, *h* transcripts are found in a band of the anterior dorsal blastoderm, extending from 85 to 95% of the egg length (EL)¹⁰.

Here we report the isolation of the pair-rule gene *paired* (*prd*) whose mutant phenotype is shown in Fig. 1. Transcripts of *prd* exhibit a pattern of seven evenly spaced bands during late syncytial blastoderm, reflecting a double-segment periodicity similar to the previously analysed pair-rule genes *ftz* and *h*. However, in contrast to the patterns of *ftz* and *h*, this pattern of *prd* transcripts is expressed only transiently and changes during cellularization of the blastoderm to a pattern with a single-segment repeat length of 14 regularly spaced bands. In addition, *prd* transcripts are detected in a dorsal band close to the anterior pole at a position similar to that seen for *h* transcripts¹⁰ and corresponding to 87 to 93% of EL.

Chromosomal walk from *esc* to *prd*

Recently, we cloned and identified the *extra sex combs* (*esc*) gene from DNA sequences at the cytogenetic locus 33B1,2 on the left arm of chromosome 2 (refs 11, 12). The initial clones,

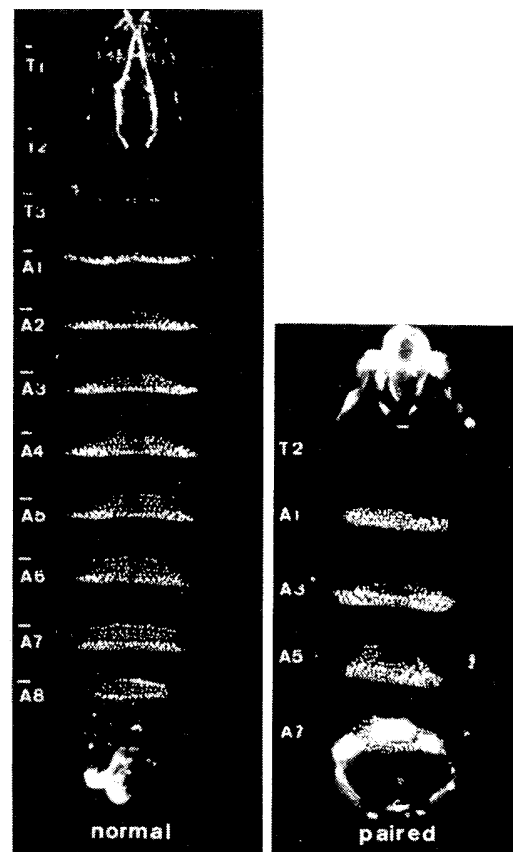


Fig. 1 Ventral cuticular pattern of a wild-type and a homozygous *prd*⁻ *Drosophila* larva. In the wild type the three thoracic (T) and eight abdominal (A) segments are indicated. In *prd*⁻, a pair-rule mutant, analogous portions of segments are deleted at a two-segment periodicity, giving rise to only half the normal number of segments¹. Because the missing portions include every other segment boundary, the segments are of a composite nature¹. For example, in the A1/A2 segment the anterior part is derived from A1, the posterior part from A2. Accordingly, the designation of segments in the *prd* mutant refers to the character of the anterior parts of the composite segments². Courtesy of C. Nüsslein-Volhard (from ref. 1).

obtained by microdissection of salivary gland chromosomes¹³, were spread over a region of 500 kilobase pairs (kb) comprising the entire deletion *Df*(2L)*esc*¹⁰. The most proximal clones, 1b.1 and 1b.8, were located just to the right of the deficiency *esc*¹⁰ and at the left end of a deficiency of *paired*, *Df*(2L)*prd*^{1,7,20} (ref. 1). The *prd* gene has been mapped previously by the deficiency

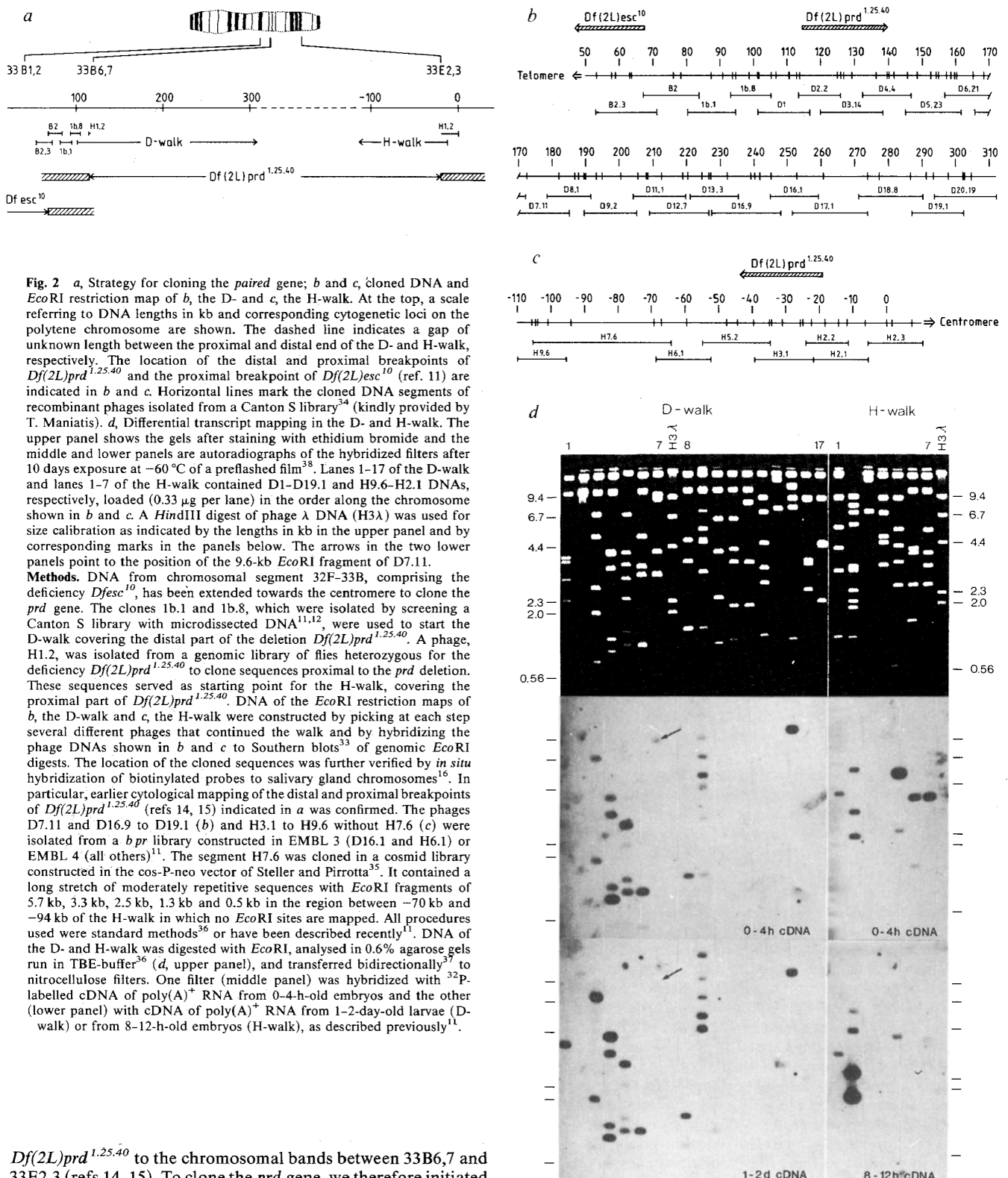


Fig. 2 *a*, Strategy for cloning the *paired* gene; *b* and *c*, cloned DNA and *Eco*RI restriction map of *b*, the D- and *c*, the H-walk. At the top, a scale referring to DNA lengths in kb and corresponding cytogenetic loci on the polytene chromosome are shown. The dashed line indicates a gap of unknown length between the proximal and distal end of the D- and H-walk, respectively. The location of the distal and proximal breakpoints of *Df(2L)prd*^{1.25.40} and the proximal breakpoint of *Df(2L)esc*¹⁰ (ref. 11) are indicated in *b* and *c*. Horizontal lines mark the cloned DNA segments of recombinant phages isolated from a Canton S library³⁴ (kindly provided by T. Maniatis). *d*, Differential transcript mapping in the D- and H-walk. The upper panel shows the gels after staining with ethidium bromide and the middle and lower panels are autoradiographs of the hybridized filters after 10 days exposure at -60°C of a preflashed film³⁸. Lanes 1-17 of the D-walk and lanes 1-7 of the H-walk contained D1-D19.1 and H9.6-H2.1 DNAs, respectively, loaded (0.33 µg per lane) in the order along the chromosome shown in *b* and *c*. A *Hind*III digest of phage λ DNA (H3λ) was used for size calibration as indicated by the lengths in kb in the upper panel and by corresponding marks in the panels below. The arrows in the two lower panels point to the position of the 9.6-kb *Eco*RI fragment of D7.11.

Methods. DNA from chromosomal segment 32F-33B, comprising the deficiency *Dfesc*¹⁰, has been extended towards the centromere to clone the *prd* gene. The clones 1b.1 and 1b.8, which were isolated by screening a Canton S library with microdissected DNA^{11,12}, were used to start the D-walk covering the distal part of the deletion *Df(2L)prd*^{1.25.40}. A phage, H1.2, was isolated from a genomic library of flies heterozygous for the deficiency *Df(2L)prd*^{1.25.40} to clone sequences proximal to the *prd* deletion. These sequences served as starting point for the H-walk, covering the proximal part of *Df(2L)prd*^{1.25.40}. DNA of the *Eco*RI restriction maps of *b*, the D-walk and *c*, the H-walk were constructed by picking at each step several different phages that continued the walk and by hybridizing the phage DNAs shown in *b* and *c* to Southern blots³³ of genomic *Eco*RI digests. The location of the cloned sequences was further verified by *in situ* hybridization of biotinylated probes to salivary gland chromosomes¹⁶. In particular, earlier cytological mapping of the distal and proximal breakpoints of *Df(2L)prd*^{1.25.40} (refs 14, 15) indicated in *a* was confirmed. The phages D7.11 and D16.9 to D19.1 (*b*) and H3.1 to H9.6 without H7.6 (*c*) were isolated from a *bpr* library constructed in EMBL 3 (D16.1 and H6.1) or EMBL 4 (all others)¹¹. The segment H7.6 was cloned in a cosmid library constructed in the cos-P-neo vector of Steller and Pirrotta³⁵. It contained a long stretch of moderately repetitive sequences with *Eco*RI fragments of 5.7 kb, 3.3 kb, 2.5 kb, 1.3 kb and 0.5 kb in the region between -70 kb and -94 kb of the H-walk in which no *Eco*RI sites are mapped. All procedures used were standard methods³⁶ or have been described recently¹¹. DNA of the D- and H-walk was digested with *Eco*RI, analysed in 0.6% agarose gels run in TBE-buffer³⁶ (*d*, upper panel), and transferred bidirectionally³⁷ to nitrocellulose filters. One filter (middle panel) was hybridized with ³²P-labelled cDNA of poly(A)⁺ RNA from 0-4-h-old embryos and the other (lower panel) with cDNA of poly(A)⁺ RNA from 1-2-day-old larvae (D-walk) or from 8-12-h-old embryos (H-walk), as described previously¹¹.

Df(2L)prd^{1.25.40} to the chromosomal bands between 33B6,7 and 33E2,3 (refs 14, 15). To clone the *prd* gene, we therefore initiated a chromosomal walk from clone 1b.8 towards the centromere (shown as the D-walk in Fig. 2*a*). Crossing the distal breakpoint of the *Df(2L)prd*^{1.25.40} deletion allowed us to clone the DNA fragment H1.2, containing sequences from both sides of the deletion (Fig. 2*a*), by screening a genomic library constructed from flies heterozygous for the deficiency *Df(2L)prd*^{1.25.40}. From proximal sequences of the clone H1.2, a second walk was then started into the *Df(2L)prd*^{1.25.40} deletion (shown as the H-walk in Fig. 2*a*). The D- and H-walks are shown in Fig. 2*b, c*. Together they cover ~300 kb of the *Df(2L)prd*^{1.25.40} deletion.

Screening for the *prd* gene

Although the converging sequences of the D- and H-walk had not joined, a screen for possible candidates of the *prd* gene by differential transcript mapping was carried out, similar to the screen that proved successful when the *esc* gene was identified^{11,12}. Radioactively labelled complementary DNAs of poly(A)⁺ RNA isolated from egg follicles, 0-4- and 8-12-h-old

embryos and 1-2-day-old larvae were hybridized to Southern blots of *EcoRI* digests of the D- and H-walk (Fig. 2d). We screened for DNA fragments that were labelled with cDNA from 0-4-h-old embryos (middle panel of Fig. 2d) but remained unlabelled when hybridized to cDNA from later stages of development (lower panel of Fig. 2d) or egg follicles (not shown). This expectation was based (1) on experiments with a temperature-sensitive *prd* allele showing zygotic expression during the blastoderm stage¹ and (2) on the absence of a maternal effect of the *prd* gene¹⁵. In the D-walk, only one such fragment was found, a 9.6-kb *EcoRI* fragment of phage D7.11 (arrows in Fig. 2d). In the H-walk, two regions at the proximal end, the 3.9-kb *EcoRI* fragment of H2.2 and the 2.6-kb *EcoRI* fragment of H3.1 (which comprises the 1.6-kb left terminal fragment of H2.2) were transcribed in 0-4-h-old embryos but not in 8-12-h-old embryos (Fig. 2d). However, these fragments of the H-walk are unlikely to harbour the *prd* gene because they are also heavily labelled by cDNA of poly(A)⁺ RNA from follicles (data not shown). Therefore, if the *prd* gene was located within the 300 kb of the *Df(2L)prd*^{1,25,40} that had already been cloned, the most likely location was the 9.6-kb *EcoRI* fragment of D7.11, at about 170-180 kb in the D-walk or 240 kb to the right of the *esc* gene^{11,12}.

Mapping the mutant *prd*^{2.45.17}

To test whether the *prd* gene was contained within the cloned 300 kb, and specifically within the 9.6-kb *EcoRI* fragment of D7.11, the D- and H-walk DNA of an X-ray-induced *prd* mutant, *prd*^{2.45.17}, was compared with that of its parent strain by whole genome Southern analysis of *EcoRI* digests. No differences were detected except for a 1.1-kb insertion into the 9.6-kb *EcoRI* fragment of D7.11 in the *prd*^{2.45.17} mutant (data not shown). The mutated DNA was isolated from a λ phage library of the heterozygous *prd*^{2.45.17} mutant, and the 4.0-kb *BamHI* fragment containing the 1.1-kb insert was subcloned. We compared its restriction map with that of the corresponding 2.9-kb *BamHI* fragment of the *prd*⁺ DNA to locate the insertion more precisely. As shown in Fig. 3, in *prd*^{2.45.17} a 1.1-kb DNA sequence has been inserted into a 0.41-kb *SmaI* fragment of the *prd* DNA. When a biotinylated probe consisting of the 1.5-kb *SmaI* fragment from *prd*^{2.45.17} (Fig. 3) was hybridized to salivary gland chromosomes¹⁶ of an Oregon R strain, it labelled more than 100 bands scattered over all chromosome arms (not shown).

Developmental profile of the *prd*⁺ transcript

Although both differential transcript mapping as well as whole genome Southern analysis suggested that the *prd* gene was located in D7.11, the possibility remained that a gene with a developmental profile similar to that of *prd* was present in D7.11 and that the 1.1-kb insert was fortuitous and did not result in an altered gene expression at its location. This objection was excluded by Northern analysis of the *prd*^{2.45.17} mutant in this region. As shown in Fig. 4, two poly(A)⁺ RNAs of 2.5 and 3.6 kb were detected in embryos of heterozygous *prd*^{2.45.17} parents whereas only a single RNA species of 2.5 kb was found in *prd*⁺ embryos. Hence, the insert in the mutant DNA is located within a transcript that exhibits the developmental profile expected for the *prd* gene. The *prd* mRNA, while absent in oocytes, accumulates to a sharp peak in 2-4-h-old embryos (blastoderm and early gastrula), followed by a precipitous decline (Fig. 4). Essentially no 2.5-kb transcripts were detectable after 12 h of embryonic development (stages after 18 h are not shown) which is consistent with the results obtained with a temperature-sensitive allele of the *prd* gene¹.

Spatial transcription pattern

Genetic analysis¹ and the developmental profile shown in Fig. 4 suggest that the main period of *prd*⁺ activity occurs around cellular blastoderm. In addition, inspection of the cuticular pattern of homozygous *prd*⁻ larvae (Fig. 1) reveals that the

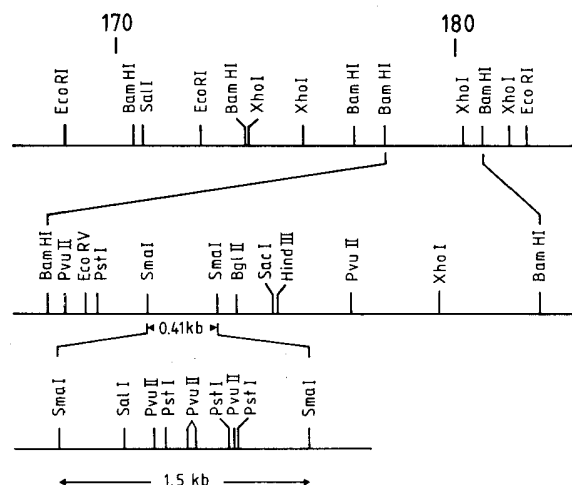


Fig. 3 Restriction map of DNA containing the *paired* gene and of *prd*^{2.45.17} mutant DNA. A restriction map of the *paired* region, obtained from D7.11, is shown at the top. Below, the 2.9-kb *BamHI* fragment, subcloned from D7.11, has been mapped in more detail. At the bottom a restriction map of the *prd*^{2.45.17} mutant DNA, containing the 1.1-kb insertion of a repetitive element, is illustrated. This region was mapped by isolating the mutated DNA from a *prd*^{2.45.17}/*prd*⁺ library according to standard methods³⁶ and mapping a subclone of the corresponding 4.0-kb *BamHI* fragment containing the inserted DNA.

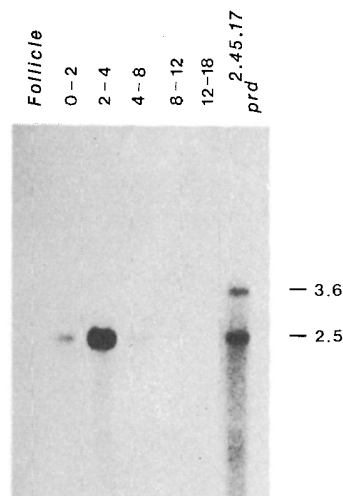


Fig. 4 Northern analysis of the *prd*⁺ and *prd*^{2.45.17} transcripts. For size calibration, end-labelled fragments of a partial *RsaI* digest of pBR322 (4.36 kb, 3.68 kb, 2.80 kb, 2.25 kb, 2.12 kb, 1.57 kb and 0.68 kb) were used (data not shown).

Methods. Poly(A)⁺ RNA (2 μ g each), isolated from wild-type egg follicles and 0-2-h, 2-4-h, 4-8-h, 8-12-h and 12-18-h-old embryos and from 0-4-h-old embryos of heterozygous *prd*^{2.45.17}/*prd*⁺ parents, as previously described¹¹, were run in a 1.1% agarose gel containing formaldehyde³⁹. The RNA was transferred in 20 \times SSC to a nitrocellulose filter according to Southern³³ and hybridized with a cDNA fragment, c73.2, nick-translated⁴⁰ with [α -³²P]dATP (3,000 Ci mmol⁻¹) and consisting of 400 base pairs (bp) at the 3' end of the *prd*⁺ transcript located to the immediate left of the 0.9-kb *BamHI* fragment (Fig. 3). The same 2.5-kb RNA was observed after hybridization with the genomic 0.9-kb *BamHI* fragment and with the genomic fragments to its left (*XhoI*-*BamHI*) and right (*PvuII*-*PvuII*), whereas no RNA was detected in a region of at least 2 kb to the right of the *XhoI* site at 180 kb (Fig. 3). A 2.3-kb cDNA clone, c7340.6, isolated from a cDNA library constructed from poly(A)⁺ RNA of 0-4-h-old embryos, spanned the same region, labelling only DNA within the 4.7-kb *XhoI* fragment between 175 and 180 kb on the genomic map (Fig. 3).

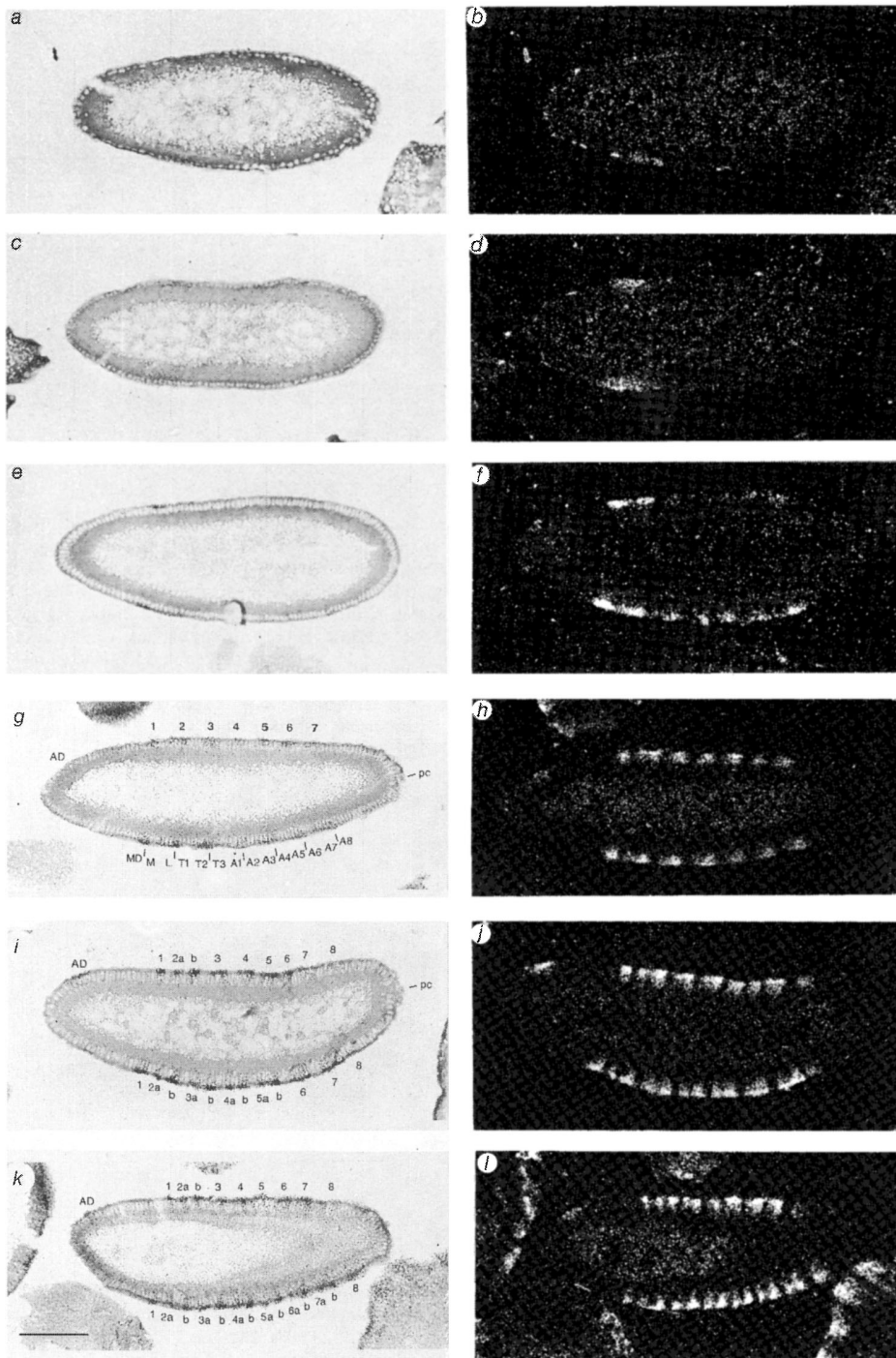


Fig. 5 Localization of *prd* transcripts in tissue sections of embryos at syncytial and cellular blastoderm. The panels show photomicrographs of the same embryos taken under phase contrast (left) or dark-field illumination (right). Sagittal or parasagittal sections through embryos during the 12th (*a, b*), 13th (*c, d*) and 14th nuclear cycle (*e-j*) of syncytial blastoderm, or at cellular blastoderm (*k, l*), are shown. Tissue sections are oriented with their dorsal side up and their anterior end to the left. The orientation was determined by morphological markers such as pole cells (pc) visible in other sections exhibiting very similar labelling. The presumptive locations of thoracic (T1-T3), abdominal (A1-A11), as well as labial (L), maxillary (M), and mandibular (MD) head segment primordia are indicated. The bands are labelled AD (anterior dorsal), 1-7 at early, and 1a-7b and 8 at late cellular blastoderm. The horizontal bar in *k* indicates a length of 0.1 mm. **Methods.** Tissue sections through young embryos were prepared, hybridized *in situ* with ^3H -labelled 2.2-kb *prd* cDNA, c7340.1 and exposed according to Hafen *et al.*⁴¹. Autoradiographic exposure was for 29 days except in *f*, which shows a 20-day exposure.

equivalent of one segment is missing for every two segments^{1,2}. From previous studies on the pair-rule genes *ftz* (ref. 8) and *h* (ref. 10), in which the structures deleted in the mutants correspond approximately to the wild-type primordia in which the genes are transcribed, we would expect *in situ* hybridizations of embryonic tissue sections with ^3H -labelled *prd*-cDNA to show a double-segment periodicity expressed at cellular blastoderm. Surprisingly, we do not observe such a strict correlation between the mutant phenotype of *prd* and the spatial distribution of its transcripts in the wild-type embryo (Fig. 5).

Localized *prd* transcripts are first observed during syncytial blastoderm (nuclear cycle 12; ref. 17) in a band 6 nuclei wide which is stronger on the ventral than on the dorsal side and

located at a distance of approximately 13 nuclei from the anterior end; that is, between 63 and 77% of EL (Fig. 5*a, b*). During the following nuclear cycle, the band widens to ~12–16 nuclei on the ventral and 8–10 nuclei on the dorsal side (Fig. 5*c, d*). It is separated by ~16–20 nuclei from the anterior pole and thus extends between 60 and 75% of EL, corresponding to the location of the primordial head segments^{6,18}. The nuclei in the anterior portion of the band are labelled more strongly than those in the posterior half. The transcripts clearly accumulate in the cortical part of the cytoplasm surrounding the nuclei, as has been observed previously for transcripts of *ftz* (ref. 8) and *h* (ref. 10). During the fourteenth nuclear cycle, at late syncytial blastoderm when nuclei begin to elongate, five additional bands

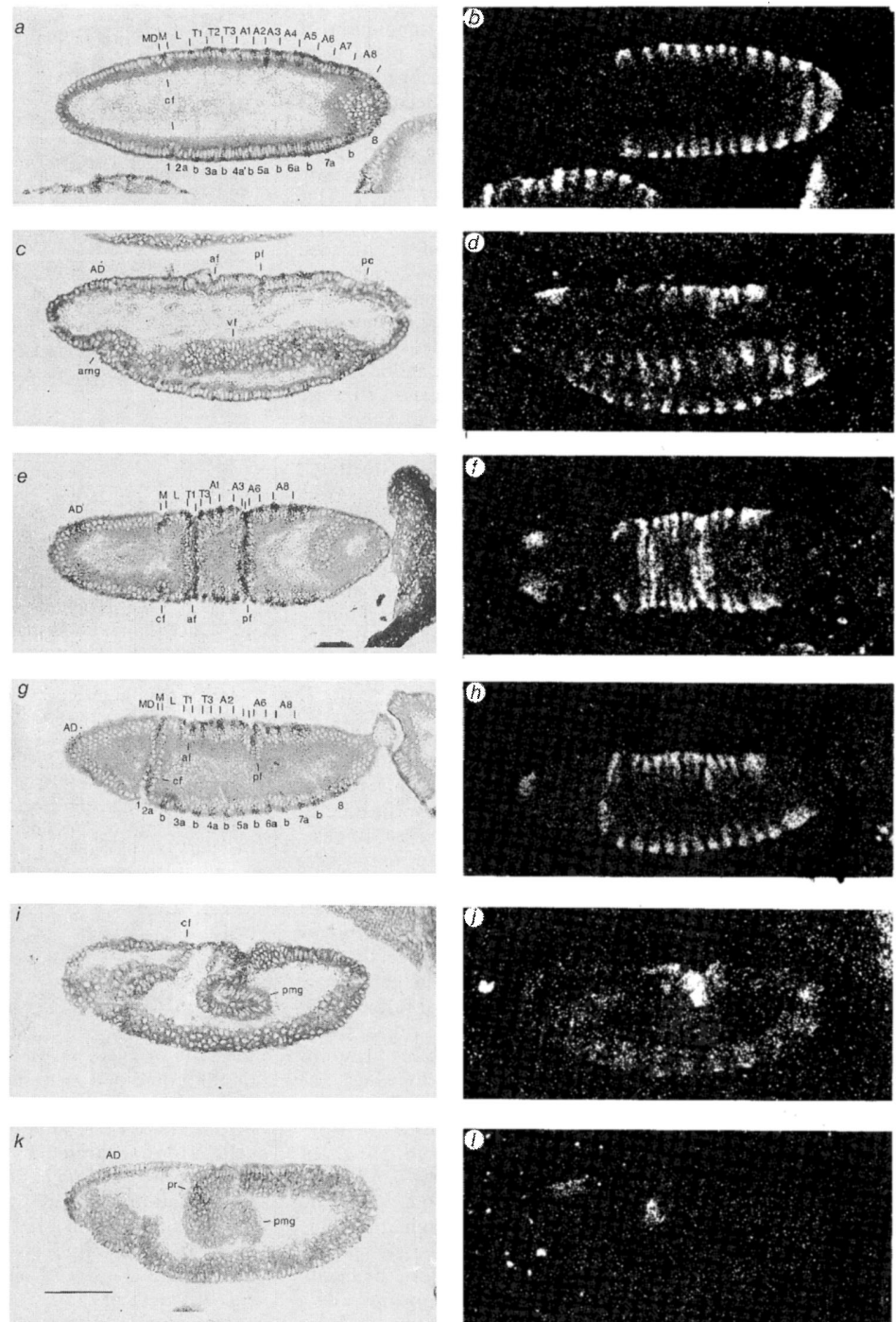


Fig. 6 Localization of *prd* transcripts in gastrulating embryos. Photomicrographs of embryonic tissue sections, prepared and treated as in Fig. 5, were taken under phase contrast (left) or dark-field illumination (right). The following developmental stages are shown: *a, b*, formation of the cephalic furrow; *c, d*, formation of the ventral furrow; *e-h*, beginning of germ-band extension at 3.5–4 h; *i, j*, germ-band extension at 4–4.5 h; *k, l*, end of germ-band extension at ~5 h development at 25 °C. The sections chosen were *a, b*, midventral and *e, f*, superficial dorsal horizontal sections; *c, d, g-l*, median or lateral sagittal sections. The anterior end is oriented to the left and, in sagittal sections, the dorsal side up. Autoradiographic exposure was for 20 days (*a-d, i-l*) or 29 days (*e-h*). The probes used for hybridization in Figs 5 and 6 comprise two short regions of the *prd* gene that are homologous with sequences elsewhere in the genome (G. Frigerio and M.N., unpublished results). However, the same patterns of hybridization are observed when a probe is used from which these *prd*-cDNA sequences have been deleted. Bands and primordial segments are labelled as in Fig. 5. The horizontal bar in *k* indicates a length of 0.1 mm. Abbreviations: af, anterior transverse fold; amg, anterior midgut; cf, cephalic furrow; pc, pole cells; pf, posterior transverse fold; pmg, posterior midgut invagination; pr, proctodeum.

of transcripts appear at approximately equal intervals. These bands are located posterior to the first band and extend to ~20% of EL, that is, to the eighth abdominal segment primordium^{6,18}. At the same time, the early anterior band splits into two bands equal in width to the five posterior bands (Fig. 5*e, f*). At this stage, therefore, *prd* transcripts occur in seven bands located between 20 and 75% of EL. The spacing of the bands is regular but closer on the dorsal than on the ventral side, and the signal intensity of the newly formed five posterior bands is again weaker dorsally than ventrally, indicating a dorso-ventral polarity of pattern development (Fig. 5*e, f*). These seven bands increase in intensity as the nuclei elongate and plasma membranes grow inwards (Fig. 5*g, h*). While the width of the posterior six bands

remains unchanged at 5–7 cells, the most anterior band is reduced in width to about four cells. This results from an elimination of transcripts in the cells of the anterior portion of the first band. In each of these six posterior bands, however, the labelling intensity is skewed in such a way that cells of the anterior half exhibit less *prd* transcripts than cells of the posterior half. The cells transcribing the *prd* gene are separated by gaps of ~2–3 cells in which no *prd* transcripts are detectable. At the same time transcripts begin to accumulate in cells located close to the anterior pole of the embryo, forming a band six cells wide (Fig. 5*g, h*) which extends between 87 and 93% of EL (Fig. 5*i, j*). In contrast to the other bands, this new band covers only the dorsal half of the embryo (Fig. 5*g-j*).

At a slightly later time, shortly before the completion of cellular blastoderm, two conspicuous events take place (Fig. 5*i, j*). First, an additional band (8) appears posterior to band 7, extending the banding pattern to ~13% of EL. Second, bands 2 to 7 begin to split into an anterior and a posterior band, a process that moves from the anterior to the posterior pole. At the stage shown in Fig. 5*i, j*, the splitting of band 2 is nearly complete whereas that of bands 6 and 7 is barely visible. This band splitting is accomplished by elimination of the transcripts in the two middle cells of each band. As a result of this process, band 2 is split into an anterior band 2a and a posterior band 2b, band 3 into 3a and 3b, and so forth. By the time of cellular blastoderm, the splitting of bands 2–7 is complete, and the width of band 1 has been further reduced from 4 to its two most posterior cells (Fig. 5*k, l*). Thus, when cellularization of the blastoderm is nearly complete, 13 bands have arisen that are about two cells wide and are separated by gaps of about two cells on the ventro-lateral side. Dorsally, splitting of the bands occurs later and is complete only in band 2 at the stage illustrated in Fig. 5*k, l*. In addition, the intensity appears to be skewed in that more transcripts accumulate in the posterior than in the anterior band. The most posterior band (8) remains unsplit and is about five cells wide. Thus, both the formation of the transcript pattern exhibiting a double-segment periodicity and its transition to one with a single-segment repeat are oriented in an anterior–posterior as well as in a ventral–dorsal direction.

Transcript distribution and morphology

To assess the morphological significance of these transcription patterns, we have attempted to relate the spatial distribution of the label to morphological features that are well known from microscope studies^{19–21}. This required an extension in time to gastrulation when such features are beginning to appear. Initially, gastrulation is marked by the formation of the ventral and cephalic furrows. As evident from Fig. 6*a, b*, the first two bands (1 and 2a) migrate into the anterior and posterior part of the cephalic furrow. In a similar manner, as the ventral furrow forms, giving rise to the mesodermal germ band, cells transcribing *prd* migrate into it. This is evident from the persistence of the banding pattern in register across the ventral furrow (Fig. 6*c, d*). Similarly, at a slightly later stage when the dorsal transverse folds appear, cells of bands coinciding with the locations of these folds move into them (Fig. 6*e–h*). At this stage, the dorsal portions of the bands have also completed their splitting (Fig. 6*e–h*). From the end of cellular blastoderm to this stage no dramatic change in band intensities is observed. However, during the next stage of germ-band extension, all bands fade with the exception of the anterior dorsal band (Fig. 6*k, l*) and the unsplit band 8, located at the proctodeal invagination (Fig. 6*i, j*). The intensity with which these two bands persists is remarkable. Only after germ-band retraction, shortly before the beginning of head involution, have these bands disappeared (data not shown).

ftz transcripts and segment primordia

Previous determinations of the positions of the *ftz* bands in the blastoderm embryo^{8,22} allow us to identify the blastoderm primordia expressing the *prd* gene. When hybridizing three consecutive sections with probes for either *prd* or *ftz*, or with both probes, we found that the pattern of *prd* transcripts is shifted to the anterior of the *ftz* bands. Whereas band 1 of *prd* does not overlap with *ftz* signals, the anterior borders of bands 2–7 (2a–7a) and band 8 of *prd* coincide with the anterior borders of bands 1–7 of *ftz* (Fig. 7). As the *ftz* bands are only about four cells wide and are spaced by gaps of about four cells^{8,10,22,23}, cells between the seven *prd* bands at late syncytial blastoderm (Fig. 5*g* and *h*) also remain unlabelled by *ftz* (data not shown). At the later stage of cellular blastoderm, when the repetitive pattern of *prd* transcripts consists of 14 bands (Figs 5*k, l*; 7*a*),

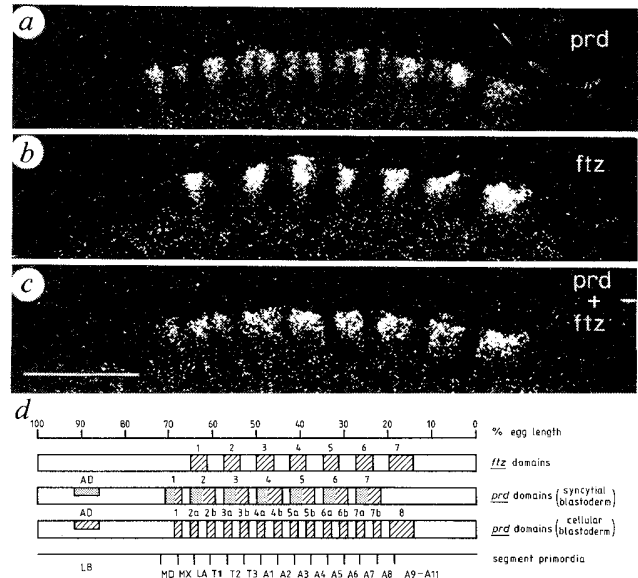


Fig. 7 Localization of *prd* relative to *ftz* transcripts. Three consecutive ventral horizontal sections through an embryo at cellular blastoderm were hybridized with *a*, ³H-labelled c7340.1 *prd* cDNA; *b*, p523B *ftz* DNA^{8,42,43}; *c*, the two probes combined and exposed for 29 days according to Hafen *et al.*⁴¹. Only one lateral side of the embryo is shown under dark-field illumination. The anterior end is oriented to the left. In *d*, the domains of *ftz* and *prd* expression are illustrated schematically relative to each other and the segment primordia. Stippled and hatched areas indicate blastoderm regions showing low and high numbers of transcripts, respectively. The *ftz* domains represented are those seen at syncytial blastoderm when they are about four nuclei wide and regularly spaced by gaps of about four nuclei^{8,22}. By the time of cellular blastoderm (*b*), *ftz* domains have been reduced in width to about three cells²². The most posterior *ftz* domain is broader and about six cells wide, as previously noted¹⁰. The horizontal bar in *c* indicates a length of 0.1 mm.

the cells of every second gap still express *ftz* (Fig. 7*b*). Thus, in the combined pattern of *prd* and *ftz* transcripts, we still observe a narrow anterior band two cells wide, consisting only of *prd* transcripts, and seven wide posterior bands, about six cells wide, separated by gaps of about two cells (Fig. 7*c*). Because the third *ftz* band covers the posterior compartment of the metathoracic and the anterior compartment of the first abdominal segment primordium^{8,22,24}, we conclude that band 4a of *prd* transcripts spans the T3/A1 segment boundary, as indicated in Figs 6*a, b* and 7*d*. If we assume that the four-cell repeat length of the *prd* banding pattern observed at this stage corresponds to the length of one segment primordium, we find that the most anterior *prd* band (1) crosses the boundary between the mandibular and maxillary segment primordia and that band 7b crosses the boundary between the seventh and eighth abdominal primordial segments (Figs 6*a, b*; 7*d*). Accordingly, the most posterior band (8) would cover the posterior compartment of A8 and probably the segment primordia of A9–A11 (Figs 6*a, b*; 7*d*). Our interpretation of the positions of the *prd* bands relative to those of *ftz* is confirmed by their relative positions with respect to the cephalic furrow. Whereas the most anterior band of *ftz* labels the posterior portion of the cephalic furrow⁸, bands 1 and 2a of *prd* are situated at its anterior and posterior edge (Fig. 6*a, b, e–h*).

Knowing how the banding pattern of *prd* RNA at early gastrula (Fig. 6*a, b*) develops from that at late syncytial blastoderm (Fig. 5*g, h*), we may trace back the location of *prd* transcripts with respect to the primordial segments at blas-

to derm. Thus, we find that the more strongly labelled posterior portions of bands 1–7 cross the boundaries between mandibular and maxillary, labial and first thoracic, second and third thoracic segment primordia, and so on, as indicated in Figs 5g, h, 7d. Similarly, we may identify segment primordia and relate them to morphological markers during later developmental stages by following the fate of cells labelled with *prd* transcripts. Accordingly, the prothoracic segment gives rise to the anterior transverse fold while the fourth and fifth abdominal segments coincide with the posterior transverse fold (Fig. 6e–h).

Discussion

Our analysis of the spatial distribution of *prd* transcripts during embryogenesis has revealed a more complex pattern than anticipated on the basis of results from previous studies with the pair-rule genes *ftz* (ref. 8) and *h* (ref. 10). Transcripts of *prd* appear first during the twelfth nuclear cycle in the region where the primordial head segments form. During subsequent nuclear divisions of the syncytial blastoderm, a pattern of seven bands builds up posteriorly along the antero-posterior axis and dorsally along the ventral-dorsal axis. At the end of this process, the *prd* pattern is similar to that of *ftz* (ref. 8) or *h* (ref. 10), showing a periodicity corresponding to two primordial segments. However, in contrast to the *ftz* and *h* patterns, the seven *prd* bands are wider and hence each covers more than one segment primordium. Thus, no simple correlation of the location of *prd* transcripts with the *prd* phenotype^{1,2} (Fig. 1) exists. To derive such a correlation, as has been possible for *ftz* (ref. 8) and *h* (ref. 10), it might be postulated that only those portions of segments are deleted in the mutant that exhibit strong transcription of the *prd* gene in the corresponding wild-type primordial segments during late syncytial blastoderm. As evident from Fig. 5g, h, these are the posterior parts of each of the seven *prd* bands, corresponding to the posterior mandibular plus anterior maxillary segment, posterior labial plus anterior first thoracic segment and so on (Fig. 7d). That this pattern of transcripts corresponds reasonably well to that of fused and deleted segments in the mutant^{1,2} (Fig. 1) may indicate that determination of segments and segment boundaries occurs already at this early stage and hence would not depend entirely on a cell-autonomous expression of *prd*.

The pattern of seven *prd* bands exists only transiently and develops during late syncytial blastoderm into a regular pattern of 13 bands of equal width and spacing. This transition of the pattern exhibiting a two-segment periodicity into one of a single-segment repeat occurs again in an anterior to posterior direction

and spreads from the ventral towards the dorsal side. Such polarities of pattern development have been observed also for *engrailed* (*en*) and *ftz* transcripts²³ and may suggest a common control mechanism. It is interesting that the pair-rule gene *prd*, initially transcribed with a two-segment repeat, is later switched to be expressed with a single-segment periodicity. Spatial expression patterns of *en* (refs 23, 25) and *ftz* (ref. 23) are also switched from longer to shorter periodicities. A switch in the pattern of *ftz* expression occurs also at a later developmental stage, as shown by the finding that the *ftz* gene product is detected in neuroblasts and ganglion cells of every segment^{26,27}. Such changes in patterns would be expected if regulatory interactions among segmentation genes occur and we anticipate that, as more of these genes are studied, more examples of such temporal changes in pattern will be discovered.

The patterns of *en* (refs 23, 28, 29) and *prd* transcripts are very similar at the end of cellular blastoderm. The two most anterior bands of both *en* (ref. 23) and *prd* label the anterior and posterior portion of the cephalic furrow. The two patterns may even coincide as *en* is probably expressed in posterior compartments of each segment^{23,28–31} and our spatial assignments of the *prd* bands are based on those of the *ftz* bands, which may be off by one cell. Thus, although *prd* and *en* are initially under different controls, as apparent from their distribution of transcripts, such a spatial and temporal coincidence of the expression of these two genes during cellular blastoderm might indicate that their control becomes at least partly coordinated at this stage.

Two additional groups of cells begin to express the *prd* gene during late syncytial blastoderm. First, transcripts appear in a dorsal band of cells close to the anterior pole at a location similar to that of *h* expression¹⁰. As has been argued previously¹⁰, these cells may represent the primordium for the labrum³². It remains to be shown, however, whether all of these cells express both *h* and *prd*. Second, a wide posterior band of *prd* transcripts that appears in the posterior region of A8 (and possibly in the primordia for A9, A10 and A11) migrates to the proctodeal invagination during germ-band extension. This band, together with the anterior dorsal band, are the last cells to exhibit *prd* expression during embryogenesis.

We thank Maya Burri for technical assistance, Christiane Nüsslein-Volhard for the *prd* mutant strains and discussions, Michael Levine for the *ftz* clone p523B, Hermann Steller for the cos-P-neo vector and Hans Noll for comments on the manuscript. This work was supported by Swiss NSF grants 3.180-0.82, 3.600-0.84 and 3.600-1.84 and by the Canton of Basel.

Received 1 October 1985; accepted 2 April 1986.

- Nüsslein-Volhard, C. & Wieschaus, E. *Nature* **287**, 795–801 (1980).
- Nüsslein-Volhard, C., Wieschaus, E. & Jürgens, G. *Verh. dt. zool. Ges.*, 91–104 (1982).
- Wieschaus, E. & Gehring, W. *Dev. Biol.* **50**, 249–263 (1976).
- Steiner, E. *Wilhelm Roux Arch. dev. Biol.* **180**, 31–46 (1976).
- Lawrence, P. A. & Morata, G. *Dev. Biol.* **56**, 40–51 (1977).
- Lohs-Schardin, M., Cremer, C. & Nüsslein-Volhard, C. *Dev. Biol.* **73**, 239–255 (1979).
- Szabad, J., Schüpbach, T. & Wieschaus, E. *Dev. Biol.* **73**, 256–271 (1979).
- Hafen, E., Kuroiwa, A. & Gehring, W. J. *Cell* **37**, 833–841 (1984).
- Holmgren, R. *EMBO J.* **3**, 569–573 (1984).
- Ingham, P. W., Howard, K. R. & Ish-Horowicz, D. *Nature* **318**, 439–445 (1985).
- Frei, E., Baumgartner, S., Edström, J.-E. & Noll, M. *EMBO J.* **4**, 979–987 (1985).
- Frei, E. *et al.* *Cold Spring Harb. Symp. quant. Biol.* **50**, 127–134 (1986).
- Scalenghe, F., Turco, E., Edström, J.-E., Pirrotta, V. & Melli, M. *Chromosoma* **82**, 205–216 (1981).
- Nüsslein-Volhard, C., Wieschaus, E. & Kluding, H. *Wilhelm Roux Arch. dev. Biol.* **193**, 267–282 (1984).
- Nüsslein-Volhard, C., Kluding, H. & Jürgens, G. *Cold Spring Harb. Symp. quant. Biol.* **50**, 145–154 (1986).
- Langer-Safer, P. R., Levine, M. & Ward, D. C. *Proc. natn. Acad. Sci. U.S.A.* **79**, 4381–4385 (1982).
- Foe, V. E. & Alberts, B. M. *J. Cell Sci.* **61**, 31–70 (1983).
- Underwood, E. M., Turner, F. R. & Mahowald, A. P. *Dev. Biol.* **74**, 286–301 (1980).
- Sonnenblick, B. P. in *Biology of Drosophila* (ed. Demerec, M.) 62–167 (Wiley, New York, 1950).
- Poulsen, D. F. in *Biology of Drosophila* (ed. Demerec, M.) 168–274 (Wiley, New York, 1950).
- Turner, F. R. & Mahowald, A. P. *Dev. Biol.* **57**, 403–416 (1977).
- Martinez-Arias, A. & Lawrence, P. A. *Nature* **313**, 639–642 (1985).
- Weir, M. P. & Kornberg, T. *Nature* **318**, 433–439 (1985).
- Akam, M. E. & Martinez-Arias, A. *EMBO J.* **4**, 1689–1700 (1985).
- DiNardo, S., Kuter, J. M., Theis, J. & O'Farrell, P. H. *Cell* **43**, 59–69 (1985).
- Carroll, S. B. & Scott, M. P. *Cell* **43**, 47–57 (1985).
- Hiromi, Y., Kuroiwa, A. & Gehring, W. J. *Cell* **43**, 603–613 (1985).
- Kornberg, T., Sidén, I., O'Farrell, P. & Simon, M. *Cell* **40**, 45–53 (1985).
- Fjose, A., McGinnis, W. J. & Gehring, W. J. *Nature* **313**, 284–289 (1985).
- Kornberg, T. *Proc. natn. Acad. Sci. U.S.A.* **78**, 1095–1099 (1981).
- Kornberg, T. *Dev. Biol.* **86**, 363–372 (1981).
- Jürgens, G., Lehmann, R., Schardin, M. & Nüsslein-Volhard, C. *Wilhelm Roux Arch. dev. Biol.* (in the press).
- Southern, E. J. *molec. Biol.* **98**, 503–517 (1975).
- Maniatis, T. *et al.* *Cell* **15**, 687–701 (1978).
- Steller, H. & Pirrotta, V. *EMBO J.* **4**, 167–171 (1985).
- Maniatis, T., Fritsch, E. F. & Sambrook, J. *Molecular Cloning: a Laboratory Manual* (Cold Spring Harbor Laboratory Press, New York, 1982).
- Smith, G. E. & Summers, M. D. *Analyt. Biochem.* **109**, 123–129 (1980).
- Laskey, R. A. & Mills, A. D. *FEBS Lett.* **82**, 314–316 (1977).
- Lehrach, H., Diamond, D., Wozney, J. M. & Boedtker, H. *Biochemistry* **16**, 4743–4751 (1977).
- Rigby, P. W. J., Dieckmann, M., Rhodes, C. & Berg, P. *J. molec. Biol.* **113**, 237–251 (1977).
- Hafen, E., Levine, M., Garber, R. L. & Gehring, W. J. *EMBO J.* **2**, 617–623 (1983).
- McGinnis, W., Levine, M. S., Hafen, E., Kuroiwa, A. & Gehring, W. J. *Nature* **308**, 428–433 (1984).
- Kuroiwa, A., Hafen, E. & Gehring, W. J. *Cell* **37**, 825–831 (1984).